



Available online at www.sciencedirect.com

ScienceDirect

Mathematics and Computers in Simulation 109 (2015) 174–185

MATHEMATICS
AND
COMPUTERS
IN SIMULATION
IMACS

www.elsevier.com/locate/matcom

Original articles

Spatial patterns through Turing instability in a reaction–diffusion predator–prey model

Lakshmi Narayan Guin *

Department of Mathematics, Visva-Bharati, Santiniketan-731 235, West Bengal, India

Received 22 November 2013; received in revised form 28 September 2014; accepted 6 October 2014

Available online 18 October 2014

Abstract

Pattern formation in nonlinear complex systems is one of the central problems of the natural, social and technological sciences. In this paper, we consider a mathematical model of predator–prey interaction subject to self as well as cross-diffusion, arising in processes described by a system of reaction–diffusion equations (coupled to a system of ordinary differential equations) exhibiting diffusion-driven instability. Spatial patterns through Turing instability in a reaction–diffusion predator–prey model around the unique positive interior equilibrium of the model are discussed. Furthermore, we present numerical simulations of time evolution of patterns subject to self as well as cross-diffusion in the proposed spatial model and find that the model dynamics exhibits complex pattern replication in the two-dimensional space. The obtained results unveil that the effect of self as well as cross-diffusion plays an important role on the stationary pattern formation of the predator–prey model which concerns the influence of intra-species competition among predators.

© 2014 International Association for Mathematics and Computers in Simulation (IMACS). Published by Elsevier B.V. All rights reserved.

Keywords: Reaction–diffusion systems; Self and cross-diffusion; Instability; Pattern formation

1. Introduction

Ecological models have been in the focus of ecological science as predation of interacting species affects population dynamics significantly. Studies on stability mechanism and the theory of spatial pattern formation through diffusion-driven instability [39] of a system of interacting populations in which a nonlinear system is asymptotically stable in the absence of diffusion but unstable in the presence of diffusion play significant role in mathematical ecology, embryology and other branches of science [3–5,18,21,24,25,28]. Spatial patterns modify the temporal dynamics and stability properties of population densities at a range of spatial scales, their effects must be incorporated in temporal ecological models that do not represent space explicitly. And the spatial component of ecological interactions has been identified as an important factor in how ecological communities are shaped [7,19,23,26,40]. In the predator–prey system models, the interaction between the predator and the prey is the reaction item and the diffusion item comes by reason of pursuit-evasion phenomenon—predators pursuing prey and prey escaping predators [1,37,38]. In such

* Tel.: +91 3463261029; fax: +91 3463261029.

E-mail address: guin.In@yahoo.com.

a system, there is a tendency that the prey stays away from the predators and the escape velocity of the preys may be taken to be proportional to the dispersive velocity of the predators. In the same manner, there is a tendency that the predators will get closer to the preys and the chase velocity of predators may be considered to be proportional to the dispersive velocity of the preys [32]. Therefore the problem of cross-diffusion arises, which was proposed first by Kerner [14] and first applied to competitive population systems by Shigesada et al. [30].

The effect of diffusion on the spatiotemporal predator–prey model has been investigated by many scientists to their insightful work [16,20,29,41]. Recently, the effect of self as well as cross-diffusion in reaction–diffusion systems has received much attention by both ecologists and mathematicians [6,9,15,31,33]. The term self-diffusion which implies the per capita diffusion rate of each species is influenced only by its own density, i.e. there is no response to the density of the other one. On the other hand, cross-diffusion implies the per capita diffusion rate of each species which is influenced not only by its own but also by the other ones density. The value of the cross-diffusion coefficient may be positive, negative or zero. The positive cross-diffusion coefficient denotes the movement of the species in the direction of lower concentration of another species while the negative cross-diffusion coefficient for one species tends to diffuse in the direction of higher concentration of another species.

In the studies of pattern formation on spatiotemporal predator–prey model with prey-dependent Holling type II functional response, little attention has been paid here to the effect of self as well as cross-diffusion, which is an extension work of the following Bazykin's [2] model:

$$\frac{du}{dt} = ru\left(1 - \frac{u}{k}\right) - \frac{auv}{u + c} = f_1(u, v), \quad (1.1a)$$

$$\frac{dv}{dt} = -dv + \frac{bu v}{u + c} - hv^2 = f_2(u, v), \quad (1.1b)$$

$$u(0) > 0, \quad v(0) > 0, \quad (1.1c)$$

where u, v denote prey and predator population size respectively at any instant of time t , and all the parameters in uniform environment viz. r, k, a, b, c, d, h are positive. The parameter r designates the intrinsic growth rate of the prey species. Similarly k denotes the carrying capacity of the prey species, a , the predation rate or capturing rate of prey by predator, b , the maximal predator growth rate, c , the interference coefficient of the predator, d , the predator natural mortality rate and h represent the predator intra-species competition.

The diffusion effect affecting the reaction–diffusion predator–prey system is one of these influent elements, modifying qualitative stability and quantitative aspects of the spatiotemporal dynamics in diffusive models. As predator–prey interactions are inherently prone to oscillations, it is therefore obvious to investigate this phenomenon as a potential mechanism for the creation of spatial patterns through Turing instability induced by self as well as cross-diffusion. However, only a few earlier works have been devoted to this issue [6,8,9,33], which is an important objective in the present work. Our present model for spatially extend systems is devoted to explain spatiotemporal behaviour of interacting populations through complex pattern replication (viz. stripe, spotted, labyrinthine or spot–stripe mixtures patterns), which concerns the influence of intra-specific competition among predators.

Intra-specific competition is a particular form of competition in which members of the same species compete for limited resources in an ecosystem (e.g. food, water, space, light, nutrients, mates or any other resource which is required for survival). This can be contrasted with inter-specific competition, in which different species compete for a shared resource. Members of the same species have very similar resources requirements whereas different species have a smaller contested resource overlap, resulting in intra-specific competition generally being a stronger force than inter-specific competition. Whenever populations of a species are crowded, intra-specific competition is intense. Intra-specific competition is a major factor affecting the carrying capacity of a population. In brief, intra-specific competition refers to a decrease in reproduction or an increase in death rate with an increase in species density [2,10–13]. In the present paper, we focus mainly on the dynamics of pattern formation in the predator–prey model with self as well as cross-diffusion effect. One of the objectives of this study is to explore the effect of diffusion and cross-diffusion coefficients on spatio-temporal dynamics in a prey-dependent predator–prey model and the novelty of this study lies with the inclusion of intra-specific competition among the predators. The rest of this paper is organized as follows. In Section 2, we introduce the model with diffusion and give the existence and feasibility criteria of the unique interior equilibrium point of (1.1). In Section 3, we discuss the results of Turing pattern formation via numerical simulations. Finally, conclusions and remarks are presented in Section 4.

2. Model with diffusion

In our present investigation, the main purpose is to investigate the spatial patterns of the system (1.1) with diffusion, admitted by the following coupled reaction–diffusion system:

$$\frac{\partial u}{\partial t} = f_1(u, v) + D_{11}\nabla^2 u + D_{12}\nabla^2 v, \quad \xi = (x, y) \in \Omega, \quad t > 0, \quad (2.1a)$$

$$\frac{\partial v}{\partial t} = f_2(u, v) + D_{21}\nabla^2 u + D_{22}\nabla^2 v, \quad \xi = (x, y) \in \Omega, \quad t > 0, \quad (2.1b)$$

$$u(0, \xi) > 0, \quad v(0, \xi) > 0, \quad \xi = (x, y) \in \Omega, \quad (2.1c)$$

$$\text{where } \nabla^2 \equiv \frac{\partial^2}{\partial \xi^2} \equiv \frac{\partial^2}{\partial x^2} + \frac{\partial^2}{\partial y^2}$$

is the usual Laplacian operator in 2-dimensional space; $\Omega \subseteq \mathbf{R}^2$ is a bounded spatial domain with smooth boundary $\partial\Omega$; D_{11} and D_{22} are the self-diffusion coefficients u and v , respectively, D_{12} and D_{21} are the cross-diffusion coefficients of v and u , respectively. Usually, diffusion is considered as a spatial transmission way, which moves from higher concentration to lower concentration and biologically, cross-diffusion means that the prey species exercise a self-defence mechanism to protect themselves from the attack of the predator. Throughout this article, we assume that $D_{11} > 0$, $D_{22} > 0$ and $D_{11}D_{22} - D_{12}D_{21} > 0$ which indicate that self diffusion is stronger than cross diffusion, i.e. the flow of the respective densities in the spatial domain depends strongly on their own density than on the others. This type of incident occurs in nature where the prey approaches towards the lower concentration of the predator in search of new food and the predator prefers to avoid group defence by a huge number of prey and chooses to catch its prey from a smaller concentration group unable to sufficiently resist.

We make a change of variables and time rescaling: $(u, v, t, x, y) = (k\tilde{u}, \frac{k b \tilde{v}}{a}, \frac{\tilde{t}}{r}, \tilde{x}L, \tilde{y}L)$, L denotes the size of the system in spatial domain Ω . For the sake of convenience, we are dropping tildes and considering zero-flux boundary conditions, model (2.1) is converted into:

$$\frac{\partial u}{\partial t} = F_1(u, v) + d_{11}\nabla^2 u + d_{12}\nabla^2 v, \quad \xi = (x, y) \in \Omega, \quad t > 0, \quad (2.2a)$$

$$\frac{\partial v}{\partial t} = F_2(u, v) + d_{21}\nabla^2 u + d_{22}\nabla^2 v, \quad \xi = (x, y) \in \Omega, \quad t > 0, \quad (2.2b)$$

$$\frac{\partial u}{\partial \nu} = \frac{\partial v}{\partial \nu} = 0, \quad \xi = (x, y) \in \partial\Omega, \quad t > 0, \quad (2.2c)$$

$$u(0, \xi) > 0, \quad v(0, \xi) > 0, \quad \xi = (x, y) \in \Omega, \quad (2.2d)$$

where $F_1(u, v) = u(1-u) - \frac{\epsilon uv}{u+\alpha}$, $F_2(u, v) = -\gamma v + \frac{\epsilon uv}{u+\alpha} - \delta v^2$ and the dimensionless parameters are $\alpha = \frac{c}{k}$, $\epsilon = \frac{b}{r}$, $\gamma = \frac{d}{r}$, $\delta = \frac{hkb}{ar}$, $d_{11} = \frac{D_{11}}{rL^2}$, $d_{12} = \frac{D_{12}b}{raL^2}$, $d_{21} = \frac{D_{21}a}{rbL^2}$, $d_{22} = \frac{D_{22}}{rL^2}$.

In addition, we assume that the diffusive matrix $D = \begin{bmatrix} d_{11} & d_{12} \\ d_{21} & d_{22} \end{bmatrix}$ is positive definite i.e. $d_{11} > 0$, $d_{22} > 0$, $d_{11}d_{22} - d_{12}d_{21} > 0$ and ν is the outward directional derivative normal to $\partial\Omega$. The main reason for choosing zero-flux boundary conditions is that we are interested in the self-organization of pattern; zero-flux conditions imply no population flux across the boundary $\partial\Omega$ [22].

To well understand patterns of the system given by (2.2), we firstly consider a spatially homogeneous system. Thus we firstly find the steady state in \mathbf{R}_+^2 as follows:

- (i) $E_0(0, 0)$, total extinction of prey and predator;
- (ii) $E_1(1, 0)$, which is corresponding to extinction of the predator;
- (iii) interior equilibrium point $E_2(u_*, v_*)$, which is corresponding to coexistence of prey and predator where $v_* = \frac{(1-u_*)(u_*+\alpha)}{\epsilon}$; $u_* \in (0, 1)$ and u_* be the root of the following cubic equation

$$p_0w^3 + 3p_1w^2 + 3p_2w + p_3 = 0, \quad (p_0 \neq 0), \quad (2.3)$$

with coefficients

$$\begin{aligned} p_0 &= \delta, \\ 3p_1 &= \delta(2\alpha - 1), \\ 3p_2 &= [\epsilon(\epsilon - \gamma) - \delta] + \delta(\alpha - 1)^2, \\ p_3 &= -(\gamma\alpha\epsilon + \delta\alpha^2). \end{aligned}$$

The converted equation of (2.3) through the transformation $z = p_0w + p_1$ is $z^3 + 3Hz + G = 0$. Eq. (2.3) has exactly one real positive root if $G^2 + 4H^3 > 0$, where $G = p_0^2 p_3 - 3p_0 p_1 p_2 + 2p_1^3$, $H = p_0 p_2 - p_1^2$ and using Cardan's method, we obtain that the root is $\frac{1}{p_0}(q - \frac{H}{q} - p_1)$, where q denotes one of the three values of $\left[\frac{(-G + \sqrt{(G^2 + 4H^3)})}{2}\right]^{\frac{1}{3}}$.

It is easy to obtain that the condition to ensure that u_* and v_* are positive is that $0 < u_* < 1$, $\alpha > \frac{1}{2}$ and $\epsilon(\epsilon - \gamma) > \delta$. From the biological point of view, we are only interested to study the dynamic behaviour around the positive interior equilibrium point $E_2(u_*, v_*)$.

3. Turing instability and pattern formation

3.1. Turing instability in the diffusion model (2.2)

In the presence of self as well as cross-diffusion, we will introduce small space and time-dependent perturbations around $E_2(u_*, v_*)$ of the system (2.2) as follows:

$$u = u_* + \bar{u}(\xi, t), \quad |\bar{u}(\xi, t)| \ll u_*, \quad (3.1a)$$

$$v = v_* + \bar{v}(\xi, t), \quad |\bar{v}(\xi, t)| \ll v_*, \quad (3.1b)$$

$$\text{with } \begin{bmatrix} \bar{u}(\xi, t) \\ \bar{v}(\xi, t) \end{bmatrix} = \begin{bmatrix} u_k \\ v_k \end{bmatrix} e^{\mu t + ik\xi}, \quad (3.1c)$$

where μ is the perturbation growth rate in time t ; u_k , v_k are the corresponding amplitudes; k is the wave-number. Substituting expression (3.1) into (2.2) and neglecting all nonlinear terms in u and v , one obtains the characteristic equation:

$$|J - k^2 D - \mu I| = 0, \quad (3.2)$$

$$J = \begin{bmatrix} 1 - 2u_* - \frac{\epsilon v_* \alpha}{(u_* + \alpha)^2} & -\epsilon u_* \\ \frac{\epsilon v_* \alpha}{(u_* + \alpha)^2} & -\gamma - 2\delta v_* + \frac{\epsilon u_*}{u_* + \alpha} \end{bmatrix} = \begin{bmatrix} \Gamma_{11} & \Gamma_{12} \\ \Gamma_{21} & \Gamma_{22} \end{bmatrix}, \quad I = \begin{bmatrix} 1 & 0 \\ 0 & 1 \end{bmatrix}.$$

The solution of the characteristic equation (3.2) is given by

$$\begin{aligned} \mu_k &= \frac{-\sigma_1 \pm \sqrt{\sigma_1^2 - 4\sigma_2}}{2}, \\ \sigma_1 &= k^2(d_{11} + d_{22}) - \text{tr}(J), \\ \sigma_2 &= \det J + k^4(d_{11}d_{22} - d_{12}d_{21}) - k^2(d_{11}\Gamma_{22} + d_{22}\Gamma_{11} - d_{12}\Gamma_{21} - d_{21}\Gamma_{12}), \\ \text{tr}(J) &= \Gamma_{11} + \Gamma_{22}, \\ \det J &= \Gamma_{11}\Gamma_{22} - \Gamma_{12}\Gamma_{21}. \end{aligned} \quad (3.3)$$

The system (2.2) will be unstable if at least one of the roots of (3.2) is positive i.e. diffusion-driven instability occurs if at least one of the conditions $\sigma_1 > 0$ and $\sigma_2 > 0$ is violated under which stationary state is unstable to spatial perturbations with $k \neq 0$. It is evident that the condition $\sigma_1 > 0$ is not violated as $\text{tr}(J) < 0$, $d_{11} > 0$ and $d_{22} > 0$. Hence, only violation of the condition $\sigma_2 > 0$ will give rise to diffusion-driven instability. To satisfy the necessary condition $\sigma_2 < 0$ for some k , the coefficient of k^2 in (3.3) must be positive i.e.

$$d_{11}\Gamma_{22} + d_{22}\Gamma_{11} - d_{12}\Gamma_{21} - d_{21}\Gamma_{12} > 0. \quad (3.4)$$

Now, we are interested to find sufficient condition in which the minimum of σ_2 is below zero. And we notice that σ_2 achieves its minimum at the critical value k_c^2 where

$$k_c^2 = \frac{d_{11}\Gamma_{22} + d_{22}\Gamma_{11} - d_{12}\Gamma_{21} - d_{21}\Gamma_{12}}{2(d_{11}d_{22} - d_{12}d_{21})}.$$

Therefore the condition $\sigma_2 < 0$ at $k^2 = k_c^2$ turns into

$$\frac{(d_{11}\Gamma_{22} + d_{22}\Gamma_{11} - d_{12}\Gamma_{21} - d_{21}\Gamma_{12})^2}{4(d_{11}d_{22} - d_{12}d_{21})} > \det J. \quad (3.5)$$

Moreover, the equation $\sigma_2 = 0$ has two positive roots k_1^2 and k_2^2 which represent the finite boundary wave numbers and satisfy the equality

$$k_{2,1}^2 = \frac{(d_{11}\Gamma_{22} + d_{22}\Gamma_{11} - d_{12}\Gamma_{21} - d_{21}\Gamma_{12}) \pm \sqrt{\Lambda}}{2(d_{11}d_{22} - d_{12}d_{21})}, \quad (3.6)$$

$$\Lambda = (d_{11}\Gamma_{22} + d_{22}\Gamma_{11} - d_{12}\Gamma_{21} - d_{21}\Gamma_{12})^2 - 4(d_{11}d_{22} - d_{12}d_{21})(\Gamma_{11}\Gamma_{22} - \Gamma_{12}\Gamma_{21}).$$

As a consequence, the following four conditions for parametric Turing space guarantee that the spatially homogeneous stable state around $E_2(u_*, v_*)$ becomes unstable to perturbation for some $k \neq 0$ ($0 < k_1^2 < k^2 < k_2^2$):

$$(i) \ tr(J) = (\Gamma_{11} + \Gamma_{22}) < 0,$$

$$\text{i.e. } (u_* + \alpha)^2 < \Lambda_1,$$

$$(ii) \ \det J = (\Gamma_{11}\Gamma_{22} - \Gamma_{12}\Gamma_{21}) > 0,$$

$$\text{i.e. } \Lambda_2 > 0,$$

$$(iii) \ (d_{11}\Gamma_{22} + d_{22}\Gamma_{11} - d_{12}\Gamma_{21} - d_{21}\Gamma_{12}) > 0,$$

$$\text{i.e. } \Lambda_3 > 0,$$

$$(iv) \ \frac{(d_{11}\Gamma_{22} + d_{22}\Gamma_{11} - d_{12}\Gamma_{21} - d_{21}\Gamma_{12})^2}{4(d_{11}d_{22} - d_{12}d_{21})} > \det J,$$

$$\text{i.e. } \Lambda_3 > 2(u_* + \alpha)\sqrt{(d_{11}d_{22} - d_{12}d_{21})\Lambda_2}, \quad \text{where}$$

$$\begin{aligned} \Lambda_1 = & 2u_*^3 + 4u_*^2\alpha + 2u_*\alpha^2 + \epsilon v_*\alpha + \gamma u_*^2 + 2\gamma u_*\alpha + \gamma\alpha^2 - \epsilon u_*^2 - \epsilon u_*\alpha + 2\delta v_*u_*^2 \\ & + 4\delta v_*u_*\alpha + 2\delta v_*\alpha^2, \end{aligned}$$

$$\begin{aligned} \Lambda_2 = & 4u_*\alpha^2\delta v_* + 2u_*\alpha^2\gamma - \alpha^2\gamma - 2\alpha^2\delta v_* + 4u_*^2\gamma\alpha + 2\alpha\epsilon v_*^2\delta - 4\alpha\delta v_*u_* + \alpha\epsilon v_*\gamma \\ & + 8u_*^2\delta v_*\alpha - 2u_*^2\alpha\epsilon + \alpha\epsilon u_* - 2\alpha\gamma u_* - 2u_*^2\delta v_* + u_*^2\epsilon - 2u_*^3\epsilon \\ & + 4u_*^3\delta v_* - u_*^2\gamma + 2u_*^3\gamma, \end{aligned}$$

$$\begin{aligned} \Lambda_3 = & -d_{11}\gamma u_*^2 - 2d_{11}\gamma u_*\alpha - d_{11}\gamma\alpha^2 + d_{11}\epsilon u_*^2 + d_{11}\epsilon u_*\alpha - 2d_{11}\delta v_*u_*^2 - 4d_{11}\delta v_*u_*\alpha \\ & - 2d_{11}\delta v_*\alpha^2 + d_{22}u_*^2 + 2d_{22}u_*\alpha + d_{22}\alpha^2 - 2d_{22}u_*^3 - 4d_{22}u_*^2\alpha - 2d_{22}u_*\alpha^2 - d_{22}\epsilon v_*\alpha \\ & - d_{12}\epsilon v_*\alpha + d_{21}\epsilon u_*^2 + d_{21}\epsilon u_*\alpha. \end{aligned}$$

The results of Fig. 1 signify that when $d_{22} > 5.03$, there is a range of values for k for which $\sigma_2 < 0$ i.e. the Turing pattern emerges, other parameter values are $\alpha = 0.3$, $\gamma = 0.2$, $\delta = 0.5$, $\epsilon = 1.0$, $d_{11} = 0.1$, $d_{12} = 0.1$, $d_{21} = 0.1$. To see the effect of cross-diffusion, we plot in Fig. 2 the dispersion relation corresponding to different values of d_{12} while keeping the others fixed. Moreover, it can be noted that the length of the interval of wave number k increases for increasing values of d_{12} .

3.2. Turing pattern structure

We execute numerical simulations of the spatially extended system (2.2) in two-dimensional space, and the qualitative results are shown here. All our numerical simulations employ the Neumann boundary conditions with a system size of 200×200 . Corresponding system parameters are captioned in the figure. We select the spatial pattern when the parameter values are in the region of Turing space. The model (2.2) in two-dimensional space is discretized using

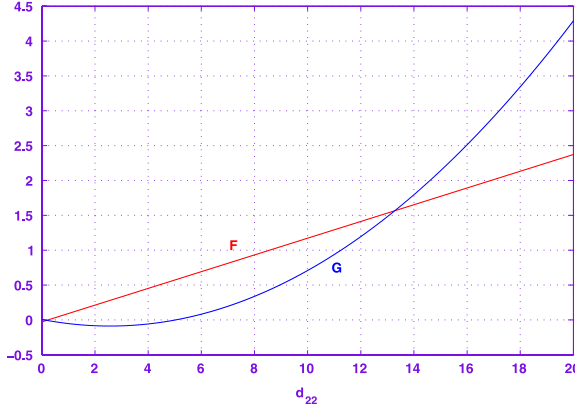


Fig. 1. Emergence of the Turing pattern corresponding to $F = [(d_{11}\Gamma_{22} + d_{22}\Gamma_{11}) - (d_{12}\Gamma_{21} + d_{21}\Gamma_{12})]$ and $G = [(d_{11}\Gamma_{22} + d_{22}\Gamma_{11}) - (d_{12}\Gamma_{21} + d_{21}\Gamma_{12})]^2 - 4(d_{11}d_{22} - d_{12}d_{21})(\det J)$.

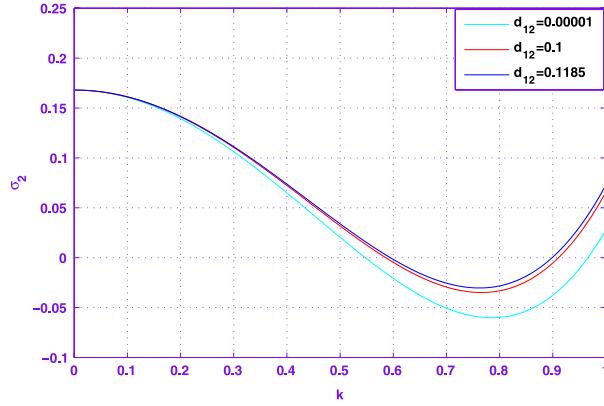


Fig. 2. Dispersion relation: plot of σ_2 for three different values of d_{12} and other system parameters are $\alpha = 0.3$, $\gamma = 0.2$, $\delta = 0.5$, $\epsilon = 1.0$, $d_{11} = 0.1$, $d_{21} = 0.1$, $d_{22} = 6.0$.

five point finite difference scheme for the spatial derivatives and solved by forward Euler scheme with time step size $dt = 0.005$ and the space step size $dx = dy = 1.0$ satisfying the CFL (Courant–Friedrichs–Lowy) stability criterion for diffusion equations [27]. It was checked that a further decrease of the step values did not lead to any significant modification of the obtained results. The initial condition is always a small amplitude random perturbation around the positive interior equilibrium $E_2(u_*, v_*)$. After the initial period during which the perturbation spreads, either the model goes into a time dependent state, or to an essentially time independent steady state solution.

We run the simulations until the patterns reach a stationary state or until the patterns show a behaviour that does not seem to change its characteristics anymore. In the proposed cross-diffusive model (2.2) through numerical simulations, various types of spatial patterns are observed and we carry on our analysis of pattern formations to the distribution of prey and predator, even if we have figured out that the distribution of prey and predator are always of the same type. Nevertheless, through the numerical simulation different types of spatiotemporal dynamics of the distribution of prey and predator are observed.

In all the cases, starting with a homogeneous steady state, the patterns take a long time to settle down, with the formation of stripe or spotted or coexistence of both patterns (cf. Figs. 3–6 and Tables 1–4). All the spatial patterns of prey and predator in these figures are generated with the initial approximation $(u_0, v_0) = (u_* + F_1(\eta), v_* + F_2(\eta))$, where $F_1(\eta) \leq 10^{-5}$ and $F_2(\eta) \leq 10^{-5}$ are spatially varying random perturbations.

Fig. 3 shows the evolution of Turing spatial pattern of prey and predator at $t = 10,000$, with small random perturbation of the stationary solution $(u_*, v_*) = (0.08194776254, 0.3684129935)$ for the system parameters $\alpha = 0.52$, $\gamma = 0.02$, $\delta = 0.5$, $\epsilon = 1.5$ and different diffusion values of the spatially homogeneous system (2.2) (cf. Table 1). One can see by comparing the relevant figures (cf. Fig. 3(a), (c), (e) and Fig. 3(b), (d), (f)) is that as d_{22} increases

Table 1

The table shows the relevant values of diffusion coefficients, time, contour pictures and species classification of Turing patterns in two-dimensional domain.

Values of diffusion coefficients	Time	Contour pictures	Species classification
$d_{11} = 0.1, d_{12} = 0.4, d_{21} = 1.8, d_{22} = 10.0$	10,000	Fig. 3(a)	prey
$d_{11} = 0.1, d_{12} = 0.4, d_{21} = 1.8, d_{22} = 10.0$	10,000	Fig. 3(b)	predator
$d_{11} = 0.1, d_{12} = 0.4, d_{21} = 1.8, d_{22} = 30.0$	10,000	Fig. 3(c)	prey
$d_{11} = 0.1, d_{12} = 0.4, d_{21} = 1.8, d_{22} = 30.0$	10,000	Fig. 3(d)	predator
$d_{11} = 0.1, d_{12} = 0.4, d_{21} = 1.8, d_{22} = 40.0$	10,000	Fig. 3(e)	prey
$d_{11} = 0.1, d_{12} = 0.4, d_{21} = 1.8, d_{22} = 40.0$	10,000	Fig. 3(f)	predator

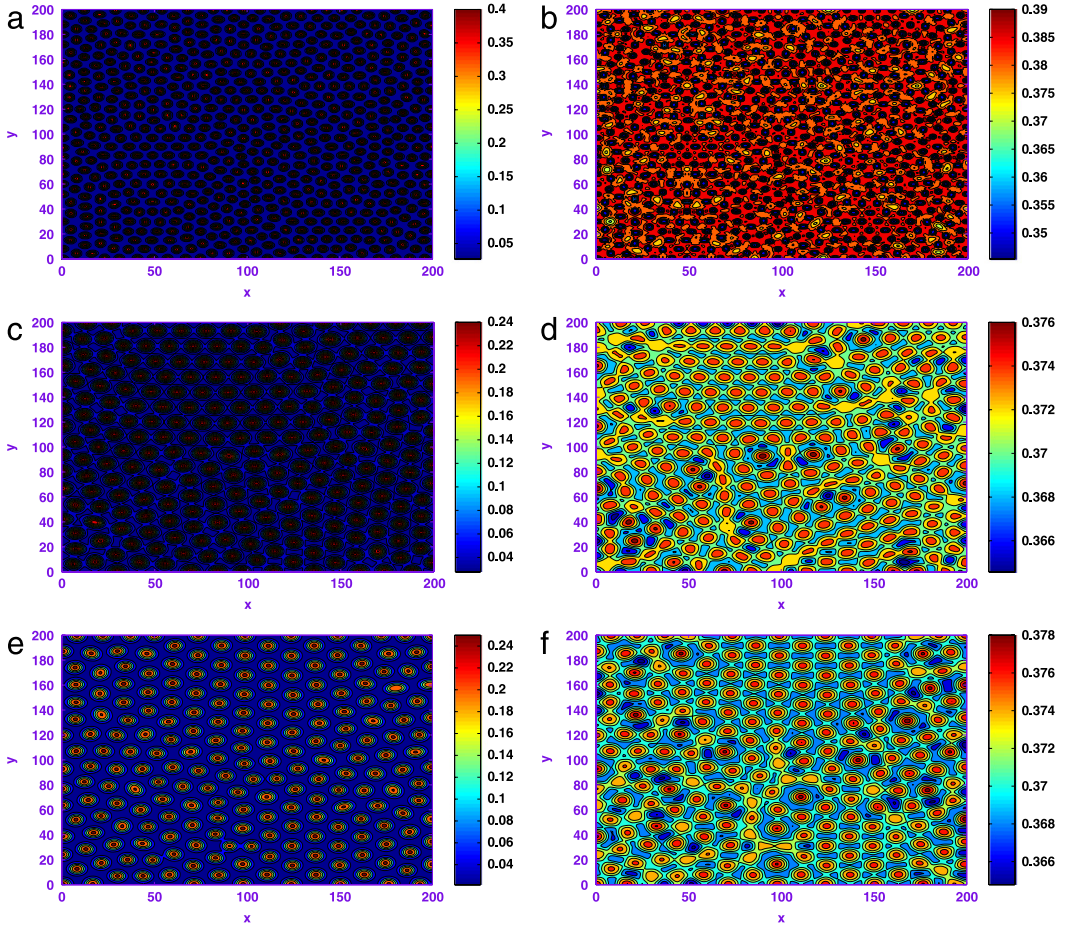


Fig. 3. Stationary Turing patterns developed by prey and predator populations in the large time for $\alpha = 0.52, \gamma = 0.02, \delta = 0.5, \epsilon = 1.5$.

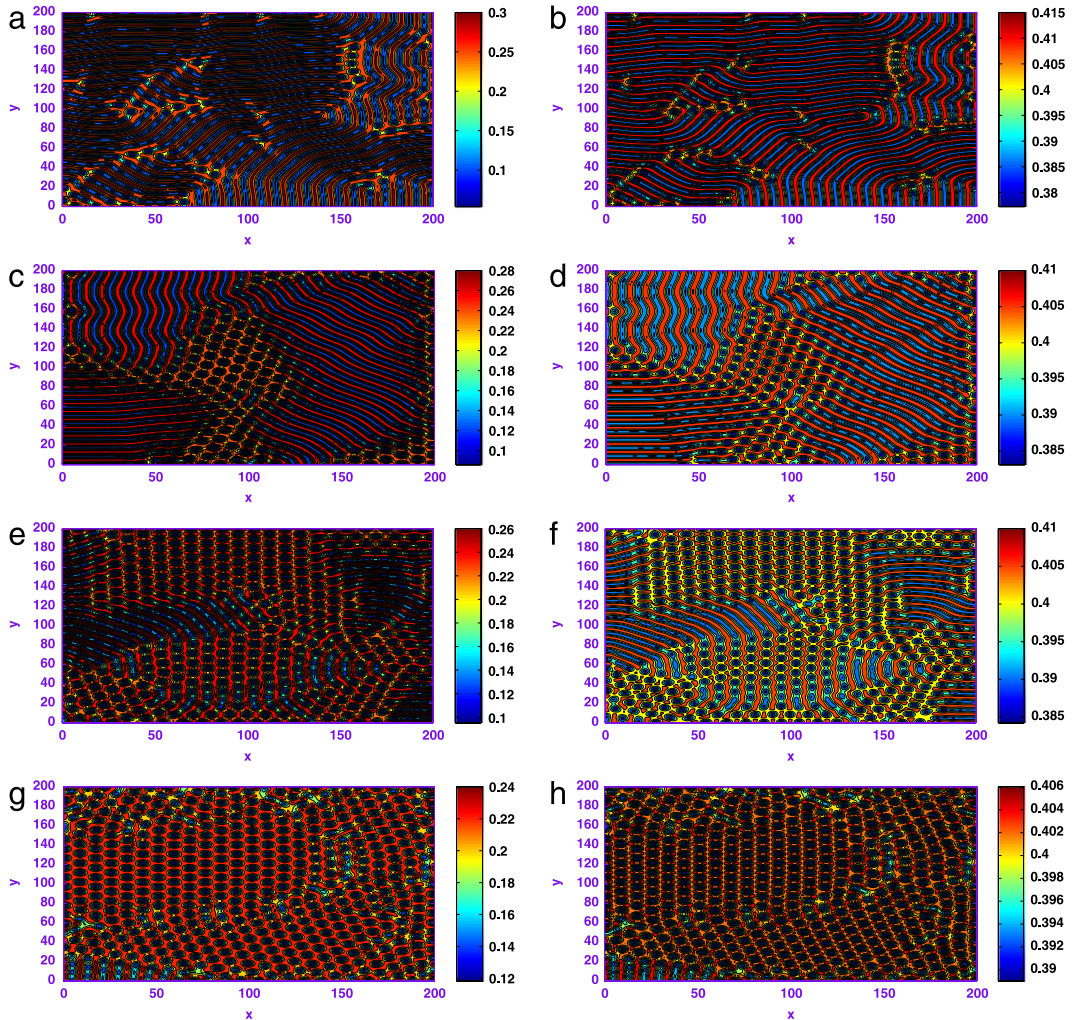
(from $d_{22} = 6.0, 30.0$ to 40.0), the diameters of the spots increase. It is also evident that the lower and the upper bounds of the prey (cf. Fig. 3(a), (c) and (e)) and predator (cf. Fig. 3(b), (d) and (f)) species within which they vary over two-dimensional space are changing with the change of d_{22} . Thus the effect of diffusion co-efficient d_{22} plays a significant role in Turing pattern formation.

In Fig. 4, we show the evolution of the spatial pattern of both the species for the spatially homogeneous system (2.2) arising out from the small random perturbation of the stationary solution $(u_*, v_*) = (0.2, 0.4)$ for several values of the cross-diffusion coefficient d_{12} (cf. Table 2) with system parameters $\alpha = 0.3, \gamma = 0.2, \delta = 0.5, \epsilon = 1.0$. From these eight panels, one can see that the regular holes and stripes spatial pattern arise from the random initial conditions. It is interesting to note that after the coexistence of regular holes and stripes pattern form, they grow steadily with time

Table 2

The table shows the relevant values of diffusion coefficients, time, contour pictures and species classification of Turing patterns in two-dimensional domain.

Values of diffusion coefficients	Time	Contour pictures	Species classification
$d_{11} = 0.1, d_{12} = 10^{-5}, d_{21} = 0.1, d_{22} = 6.0$	10,000	Fig. 4(a)	prey
$d_{11} = 0.1, d_{12} = 10^{-5}, d_{21} = 0.1, d_{22} = 6.0$	10,000	Fig. 4(b)	predator
$d_{11} = 0.1, d_{12} = 0.1185, d_{21} = 0.1, d_{22} = 6.0$	10,000	Fig. 4(c)	prey
$d_{11} = 0.1, d_{12} = 0.1185, d_{21} = 0.1, d_{22} = 6.0$	10,000	Fig. 4(d)	predator
$d_{11} = 0.1, d_{12} = 0.15, d_{21} = 0.1, d_{22} = 6.0$	10,000	Fig. 4(e)	prey
$d_{11} = 0.1, d_{12} = 0.15, d_{21} = 0.1, d_{22} = 6.0$	10,000	Fig. 4(f)	predator
$d_{11} = 0.1, d_{12} = 0.2, d_{21} = 0.1, d_{22} = 6.0$	10,000	Fig. 4(g)	prey
$d_{11} = 0.1, d_{12} = 0.2, d_{21} = 0.1, d_{22} = 6.0$	10,000	Fig. 4(h)	predator

Fig. 4. Dynamic spatiotemporal patterns developed by prey and predator populations at different instants for $\alpha = 0.3, \gamma = 0.2, \delta = 0.5, \epsilon = 1.0$.

and ending with regular holes pattern only (cf. Fig. 4(g) and (h)); and the dynamics of the system does not undergo any further changes.

When d_{21} is being increased from $d_{21} = 0.1$ to $d_{21} = 0.2$ and $d_{21} = 0.3$ (cf. Table 3), we show the snapshots of prey and predator spatial pattern at stationary level in Fig. 5. Although the dynamics of the system starts from the same

Table 3

The table shows the relevant values of diffusion coefficients, time, contour pictures and species classification of Turing patterns in two-dimensional domain.

Values of diffusion coefficients	Time	Contour pictures	Species classification
$d_{11} = 0.1, d_{12} = 0.1, d_{21} = 0.1, d_{22} = 6.0$	10,000	Fig. 5(a)	prey
$d_{11} = 0.1, d_{12} = 0.1, d_{21} = 0.1, d_{22} = 6.0$	10,000	Fig. 5(b)	predator
$d_{11} = 0.1, d_{12} = 0.1, d_{21} = 0.2, d_{22} = 6.0$	10,000	Fig. 5(c)	prey
$d_{11} = 0.1, d_{12} = 0.1, d_{21} = 0.2, d_{22} = 6.0$	10,000	Fig. 5(d)	predator
$d_{11} = 0.1, d_{12} = 0.1, d_{21} = 0.3, d_{22} = 6.0$	10,000	Fig. 5(e)	prey
$d_{11} = 0.1, d_{12} = 0.1, d_{21} = 0.3, d_{22} = 6.0$	10,000	Fig. 5(f)	predator

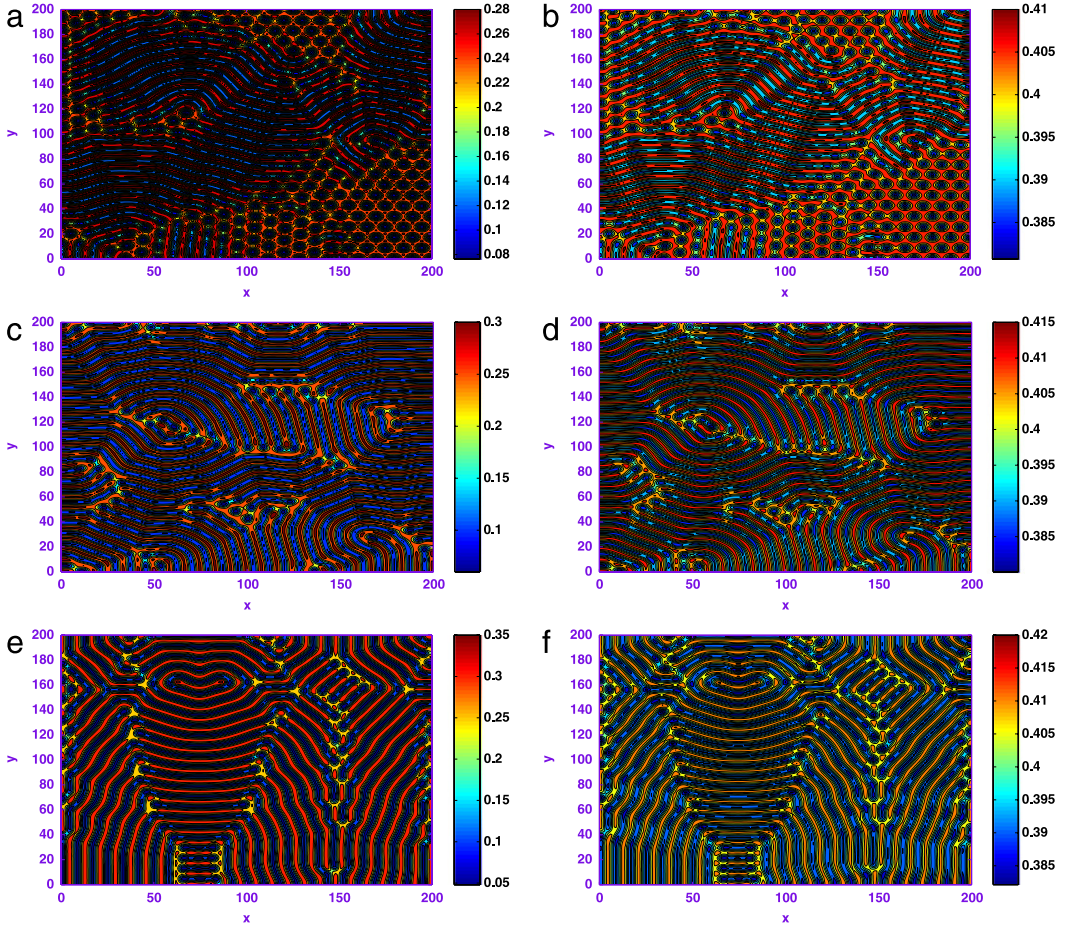


Fig. 5. Dynamic spatiotemporal patterns developed by prey and predator populations at different instants for $\alpha = 0.3, \gamma = 0.2, \delta = 0.5, \epsilon = 1.0$.

initial condition as the previous case, there is an essential difference for the spatially extended model. From these six panels of Fig. 5, one can see that the regular holes and stripes spatial pattern arise and they coexist almost equally in the spatial domain from the random perturbation of the stationary solution u_* and v_* . After the coexistence of regular holes and stripes pattern form, they grow steadily with time and stripes pattern prevail over the whole domain at last (cf. Fig. 5(e) and (f)); and the dynamics of the system does not undergo any further changes. However, with the increase of the value of d_{21} (from $d_{21} = 0.1$ to 0.3), the population density in stripes pattern becomes relatively high. Thus the effect of cross-diffusion co-efficient d_{21} plays an important role in Turing pattern formation.

Fig. 6 shows the evolution of the spatial pattern of interacting populations in the case of self-diffusion (i.e. $d_{12} = 0.0, d_{21} = 0.0$) at $t = 5000$, with small random perturbation around the stationary solution (u_*, v_*) of the spatially

Table 4

The table shows the relevant values of diffusion coefficients, time, contour pictures and species classification of Turing patterns in two-dimensional domain.

Values of diffusion coefficients	Time	Contour pictures	Species classification
$d_{11} = 0.1, d_{12} = 0.0, d_{21} = 0.0, d_{22} = 6.0$	5000	Fig. 6(a)	prey
$d_{11} = 0.1, d_{12} = 0.0, d_{21} = 0.0, d_{22} = 6.0$	5000	Fig. 6(b)	predator
$d_{11} = 0.1, d_{12} = 0.0, d_{21} = 0.0, d_{22} = 10.0$	5000	Fig. 6(c)	prey
$d_{11} = 0.1, d_{12} = 0.0, d_{21} = 0.0, d_{22} = 10.0$	5000	Fig. 6(d)	predator
$d_{11} = 0.1, d_{12} = 0.0, d_{21} = 0.0, d_{22} = 40.0$	5000	Fig. 6(e)	prey
$d_{11} = 0.1, d_{12} = 0.0, d_{21} = 0.0, d_{22} = 40.0$	5000	Fig. 6(f)	predator

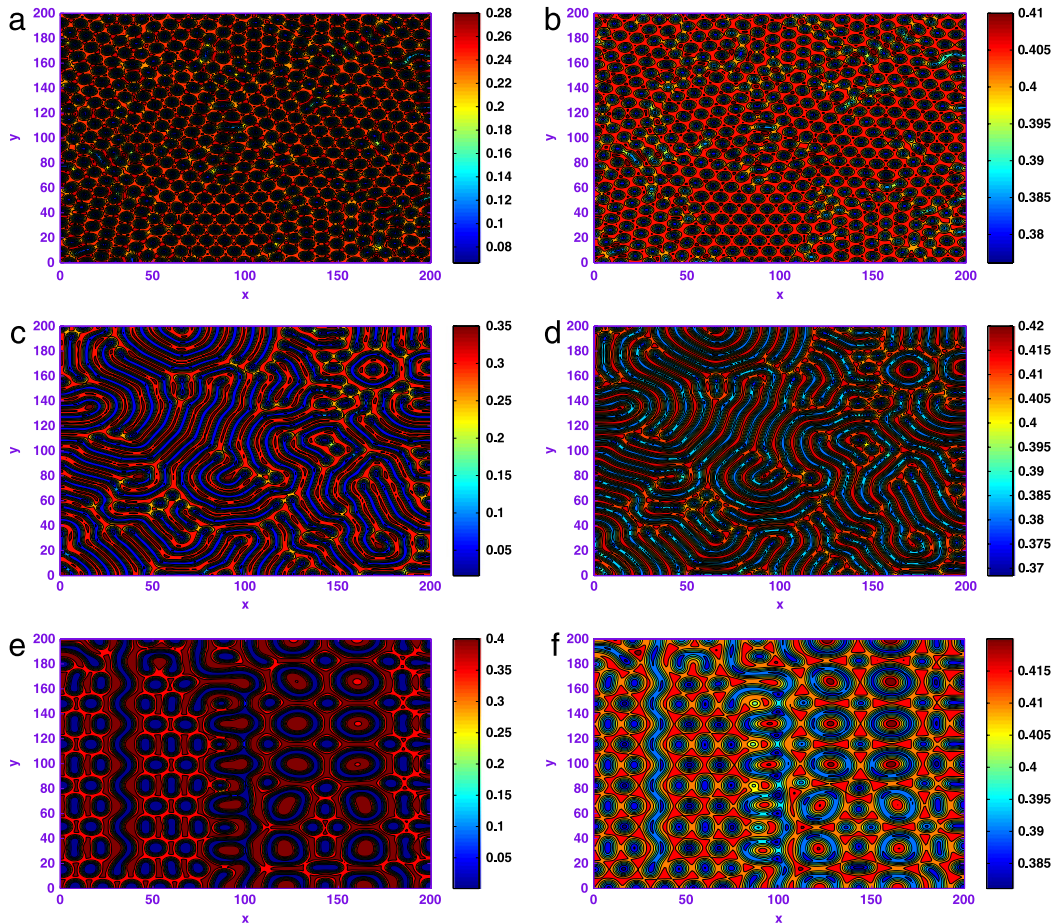


Fig. 6. Dynamic spatiotemporal patterns developed by prey and predator populations at different instants for $\alpha = 0.3, \gamma = 0.2, \delta = 0.5, \epsilon = 1.0$.

homogeneous systems (cf. Table 4). In that case, one observes that the holes pattern (cf. Fig. 6(a, b)) developed from the Turing instability corresponding to $d_{11} = 0.1, d_{22} = 6.0$, changes to labyrinthine pattern (cf. Fig. 6(c, d)) for $d_{11} = 0.1, d_{22} = 10.0$. Finally, holes pattern, spots pattern with blue ring and stripes pattern (cf. Fig. 6(e, f)) emerge for $d_{11} = 0.1, d_{22} = 40.0$ in the spatially extended model (2.2), and dynamics of the system does not undergo any further changes.

Ecologically speaking, spots pattern shows that the prey population are driven by predators to a high level in those regions, while holes pattern shows that the prey population are driven by predators to a very low level in those regions. For the survival of predator-prey species, diffusion of prey in the direction of lower concentration predator and the diffusion of predator in the direction of higher concentration of prey is common in nature. But in real ecology, it

has been observed that predator try to avoid the group defence by the large number of prey and chooses to catch its prey from a smaller group unable to sufficiently resist. Throughout this investigation, we have considered the positive cross diffusions i.e., the movement of the species in the direction of lower concentration of another species that leads to uniform steady state unstable. It seems that cross-diffusion is able to generate various spatiotemporal patterns through diffusion-driven instability. Therefore, one can predict that the effect of self as well as cross-diffusion can be considered as an important mechanism for the appearance of complex spatiotemporal patterns in spatial predator-prey system.

4. Conclusions and remarks

System (2.2) describes the dynamics of a Holling type II functional response predator-prey interaction in the form of logistic population growth in prey and intra-species competition among predators with diffusion which always exists in nature. Through mathematical analysis and numerical simulations, we obtain a parametric Turing space where various spatiotemporal patterns namely, stripe, spotted, labyrinthine or spot-stripe mixtures patterns emerge. It is believed that the observations made in this investigation related to self as well as cross-diffusion effect in spatial predator-prey system remind us of the importance of the diffusion effect. On the other hand, in this paper, the bifurcation analysis and numerical computation unveil that we can observe Turing patterns including complex patterns replication, which are similar phenomena that Wang et al. in [40] explored into a ratio dependent predator-prey model.

Therefore, our present model for spatially extended systems could be useful to explain spatiotemporal behaviour of interacting populations whose dynamics is affected by diffusion. This theoretical investigation suggests in carrying out specific experiments: intra-specific competition among predators acts as an underlying mechanism able to produce non-uniform spatial distributions of predators and prey through Turing instability. The intra-specific competition among the predator species is one of the most convincing mechanisms for the spontaneous generation of patterns in a homogeneous environment. A significant amount of work is required in support of intra-specific competition. The results of this investigation possess significance as an important step towards providing some conceptual ideas in the theoretical biology community with simple practical methods, for an in-depth study of the key dynamics of realistic predator-prey model. However, in the present paper, the obtained results show that the interaction of self-diffusion and cross-diffusion plays an important role on the pattern formation of proposed predator-prey model. The most important observation is that the Turing instability can be induced by cross-diffusion, which shows that the system dynamics exhibits complex pattern replication controlled by the cross-diffusion.

Nature is much more complex than models and also laboratories. The deterministic environment is rarely the case in real life. Natural environments are random environments, therefore the inclusion of noise sources in the proposed mathematical model (2.2) could give more realistic results from physical point of view [34,17,35]. On the other hand, incorporation of migration is also an important concept in population dynamics [36]. This is desirable in future studies.

Thus, we believe that the obtained results related to predator-prey interactions with self as well as cross-diffusion effect will be useful to theoretical mathematicians and ecologists who are engaged in performing experimental work.

Acknowledgments

The author would like to thank the anonymous reviewers for their valuable comments and suggestions, which are very helpful in the revision of the paper. I am greatly indebted to Prof. Santabrata Chakravarty and Prof. Prashanta Kumar Mandal, Department of Mathematics, Visva-Bharati for their very helpful discussion. The author gratefully acknowledges the financial support in part from Special Assistance Programme (SAP-II) sponsored by the ‘University Grants Commission (UGC), New Delhi, India’.

References

- [1] S. Aly, I. Kim, D. Sheen, Turing instability for a ratio-dependent predator-prey model with diffusion, *Appl. Math. Comput.* 217 (2011) 7265–7281.
- [2] A.D. Bazykin, A.I. Khibnik, B. Krauskopf, *Nonlinear Dynamics of Interacting Populations*, World Scientific, Singapore, 1998.
- [3] L. Chen, A. Jüngel, Analysis of a parabolic cross-diffusion semiconductor model with electron-hole scattering, *Comm. Partial Differential Equations* 32 (2007) 127–148.
- [4] G.C. Cruywagen, J.D. Murray, P.K. Maini, Biological pattern formation on two-dimensional spatial domains: a nonlinear bifurcation analysis, *SIAM J. Appl. Math.* 57 (1997) 1485–1509.

- [5] D. Del-Castillo-Negrete, B.A. Carreras, V. Lynch, Front propagation and segregation in a reaction–diffusion model with cross-diffusion, *Phys. D* 168 (2002) 45–60.
- [6] B. Dubey, B. Das, J. Hussain, A predator–prey interaction model with self and cross-diffusion, *Ecol. Model.* 141 (2001) 67–76.
- [7] M.R. Garvie, Finite-difference schemes for reaction–diffusion equations modeling predator–prey interactions in MATLAB, *Bull. Math. Biol.* 69 (2007) 931–956.
- [8] L.N. Guin, Existence of spatial patterns in a predator–prey model with self- and cross-diffusion, *Appl. Math. Comput.* 226 (2014) 320–335.
- [9] L.N. Guin, M. Haque, P.K. Mandal, The spatial patterns through diffusion-driven instability in a predator–prey model, *Appl. Math. Model.* 36 (2012) 1825–1841.
- [10] L.N. Guin, P.K. Mandal, Spatial pattern in a diffusive predator–prey model with sigmoid ratio-dependent functional response, *Int. J. Biomath.* 7 (2014) 1450047:(1–26).
- [11] M. Haque, Ratio-dependent predator–prey models of interacting populations, *Bull. Math. Biol.* 71 (2009) 430–452.
- [12] M. Haque, Existence of complex patterns in the Beddington–Deangelis predator–prey model, *Math. Biosci.* 239 (2012) 179–190.
- [13] M. Haque, A detailed study of the Beddington–Deangelis predator–prey model, *Math. Biosci.* 234 (2011) 1–16.
- [14] E.H. Kerner, Further considerations on the statistical mechanics of biological associations, *Bull. Math. Biophys.* 21 (1959) 217–255.
- [15] X. Lian, Y. Yue, H. Wang, Pattern formation in a cross-diffusive ratio-dependent predator–prey model, *Discrete Dyn. Nat. Soc.* (2012), <http://dx.doi.org/10.1155/2012/814069>.
- [16] Z.Z. Li, M. Gao, C. Hui, X.Z. Han, H. Shi, Impact of predator pursuit and prey evasion on synchrony and spatial patterns in metapopulation, *Ecol. Model.* 185 (2005) 245–254.
- [17] L. Li, Z. Jin, Pattern dynamics of a spatial predator–prey model with noise, *Nonlinear Dynam.* 67 (2012) 1737–1744.
- [18] R.M. May, Stability and Complexity in Model Ecosystems, Princeton University Press, 2001.
- [19] A.B. Medvinsky, S.V. Petrovskii, I.A. Tikhonova, H. Malchow, B.L. Li, Spatiotemporal complexity of plankton and fish dynamics, *SIAM Rev.* 44 (2002) 311–370.
- [20] A. Morozov, S. Petrovskii, B.L. Li, Spatiotemporal complexity of patchy invasion in a predator–prey system with the Allee effect, *J. Theoret. Biol.* 238 (2006) 18–35.
- [21] J.D. Murray, Mathematical Biology, Springer-Verlag, Berlin, 1993.
- [22] J.D. Murray, Discussion: Turing’s theory of morphogenesis—its influence on modelling biological pattern and form, *Bull. Math. Biol.* 52 (1990) 119–152.
- [23] C. Neuhauser, Mathematical challenges in spatial ecology, *Notices Amer. Math. Soc.* 48 (2001) 1304–1314.
- [24] A. Okubo, Diffusion and Ecological Problems: Mathematical Models, Springer-Verlag, Berlin (FRG), 1980.
- [25] A. Okubo, S.A. Levin, Diffusion and Ecological Problems: Modern Perspective, Springer-Verlag, 2001.
- [26] L.A. Segel, J.L. Jackson, Dissipative structure: an explanation and an ecological example, *J. Theoret. Biol.* 37 (1972) 545–559.
- [27] J. Shen, Y.M. Jung, Geometric and stochastic analysis of reaction–diffusion patterns, *Int. J. Pure Appl. Math.* 19 (2005) 195–244.
- [28] J.A. Sherratt, Wavefront propagation in a competition equation with a new motility term modelling contact inhibition between cell populations, *Proc. R. Soc. Lond. Ser. A Math. Phys. Eng. Sci.* 456 (2000) 2365–2386.
- [29] J.A. Sherratt, M.J. Smith, Periodic travelling waves in cyclic populations: field studies and reaction–diffusion models, *J. R. Soc. Interface* 5 (2008) 483–505.
- [30] N. Shigesada, K. Kawasaki, E. Teramoto, Spatial segregation of interacting species, *J. Theoret. Biol.* 79 (1979) 83–99.
- [31] J. Shi, Z. Xie, K. Little, Cross-diffusion induced instability and stability in reaction–diffusion systems, *J. Appl. Anal. Comput.* 1 (2011) 95–119.
- [32] J.B. Shukla, S. Verma, Effects of convective and dispersive interactions on the stability of two species, *Bull. Math. Biol.* 43 (1981) 593–610.
- [33] G.Q. Sun, Z. Jin, L. Li, M. Haque, B.L. Li, Spatial patterns of a predator–prey model with cross diffusion, *Nonlinear Dynam.* 69 (2012) 1631–1638.
- [34] G.Q. Sun, Z. Jin, L. Li, Q.X. Liu, The role of noise in a predator–prey model with Allee effect, *J. Biol. Phys.* 35 (2009) 185–196.
- [35] G.Q. Sun, Z. Jin, Q.X. Liu, B.L. Li, Rich dynamics in a predator–prey model with both noise and periodic force, *BioSyst.* 100 (2010) 14–22.
- [36] G.Q. Sun, Z. Jin, Q.X. Liu, L. Li, Dynamical complexity of a spatial predator–prey model with migration, *Ecol. Model.* 219 (2008) 248–255.
- [37] G.Q. Sun, S. Sarwardi, P.J. Pal, S. Rahman, The spatial patterns through diffusion-driven instability in modified Leslie–Gower and Holling-type II predator–prey model, *J. Biol. Systems* 18 (2010) 593–603.
- [38] G.Q. Sun, G. Zhang, Z. Jin, L. Li, Predator cannibalism can give rise to regular spatial pattern in a predator–prey system, *Nonlinear Dynam.* 58 (2009) 75–84.
- [39] A.M. Turing, The chemical basis of morphogenesis, *Philos. Trans. R. Soc. Lond. Ser. B Biol. Sci.* 237 (1952) 37–72.
- [40] W. Wang, Q.X. Liu, Z. Jin, Spatiotemporal complexity of a ratio-dependent predator–prey system, *Phys. Rev. E* 75 (2007) 051913:(1–9).
- [41] X.C. Zhang, G.Q. Sun, Z. Jin, Spatial dynamics in a predator–prey model with Beddington–Deangelis functional response, *Phys. Rev. E* 85 (2012) 021924:(1–14).